JOURNAL OF SOLID STATE CHEMISTRY 101, 77–86 (1992)

Electrical Conductivity and Metal–Nonmetal Transition in the Perovskite-Related Layered System $Ca_{n+1}Ti_nO_{3n+1-\delta}$ (n = 2, 3, and ∞)

IN-SEON KIM, MITSURU ITOH, AND TETSURŌ NAKAMURA

Research Laboratory of Engineering Materials, Tokyo Institute of Technology, 4259 Nagatuta-cho, Midori-ku, Yokohama 227, Japan

Received December 26, 1991; in revised form April 13, 1992; accepted April 16, 1992

A series of dielectric compounds having perovskite-related structures $Ca_3Ti_2O_7$, $Ca_4Ti_3O_{10}$, and $CaTiO_3$ with the general formula $Ca_{n+1}Ti_nO_{3n+1}$ (n = 2, 3, and ∞) showed a metallic conductivity when electron carriers were doped by reduction under H_2 atmosphere. The temperature dependence of the metallic resistivity up to 300 K was found to be a linear function of T^2 in a wide temperature region. The system showed a metal–nonmetal transition as a function of temperature below 120 K. An activation type hopping conduction was observed down to a few tens kelvin, and a variable range hopping conduction below that temperature was observed. The electrical transport phenomena of the system showed a strong dependence on the oxygen deficiency δ, but little dependence of the stacking number of the perovskite slab n.

Introduction

Doping with electrons or holes in the perovskite-related oxides attracts our attention because of the possibility of oxide superconductivity. Reduced $SrTiO_3$ is the well-known example, where the importance of electron doping in a d-orbital of a nonmetallic system has been shown (*1*). In this paper we report the transport phenomena of the reduced $Ca_{n+1}Ti_nO_{3n+1}$ compounds, that is, $Ca_3Ti_2O_7$ for n = 2, $Ca_4Ti_3O_{10}$ for n = 3, and $CaTiO_3$ for n = ∞. These compounds are members of the Ruddlesdon–Popper-type layered compounds with the general formula $AO(ABO_3)_n$ for n = 1, 2, 3, and ∞ (*2*). The ABO_3 perovskite is the end member of the series for n = ∞. The other end member of this series, A_2BO_4 for n = 1, is known as a K_2NiF_4-type compound, whose crystal structure is built from an alternate stacking of a perovskite slab and a rock-salt slab. The structure of the midmember n = 2 or n = 3, respectively, is built from an insertion of two or three layers of perovskite slabs $(ABO_3)_n$ between the single layers of a rock-salt slab AO. In the Ca–Ti–O system, only the compounds with n = 2, 3, and ∞, i.e., $Ca_3Ti_2O_7$, $Ca_4Ti_3O_{10}$, and $CaTiO_3$, are known (*3*).

The electrical conductivity of the perovskite oxides is distributed over a very wide range. For example, some of the oxides are good conductors with resistivity less than 10^{-5} Ω cm, whereas some others are good insulators with resistivity greater than 10^{12} Ω cm. There are several review articles in which the conductivities of perovskite oxide compounds are compiled (*4, 5*). However, the fundamental electronic states or

0022-4596/92 $5.00

energies that determine why some oxides are metallic and some are insulating remain to be elucidated. The metallic oxides, excluding superconducting states, generally have an electrical conductivity lower than that of metals, even though they have the same order of carrier density.

The shift from three-dimensional to two-dimensional linkage of BO_6 octahedra in the perovskite-slab compounds $AO(ABO_3)_n$ plays an important role in their electronic conductivity. For example, the three-dimensional perovskites $SrVO_3$, $BaPbO_3$, and $SrRuO_3$ show metallic conductivity, while the two-dimensional oxides Sr_2VO_4, Ba_2PbO_4, and Sr_2RuO_4 show nonmetallic conductivity (6). Such a dimensionality of BO_6 linkage can be an interesting parameter in addition to the conventional parameters of temperature, pressure, electric and magnetic fields, composition, distribution of components, etc., which influence the nature of the metal–nonmetal transition (*7*).

We are interested in the electrical transport phenomena of the electron-doped insulating oxides, especially perovskite oxides. The reduced perovskites (Ca, Sr, or Ba)TiO_{3-x} or doped $SrTiO_3$ (for example, Ni-doped) show various drastic electrical transport phenomena in contrast with those of the stoichiometric compounds with highly resistive and dielectric behaviors (*8*). We can also expect the structural shift from the two-dimensional A_2BO_4 to the three-dimensional ABO_3 to have an effect on the electrical transport phenomena or metal–nonmetal transition for the perovskite-slab compounds $AO(ABO_3)_n$. Among Ca, Sr, and Ba compounds, only Ca and Sr compounds have layered structures. In the case of $Sr_{n+1}Ti_nO_{3n+1}$, the $n = 3$ compound $Sr_4Ti_3O_{10}$ has been very difficult to synthesize (*9*), and the two-dimensional compound Sr_2TiO_4 has been very difficult to dope with electrons using our reducing apparatus. Thus, we have chosen the $Ca_{n+1}Ti_nO_{3n+1-\delta}$ compounds and studied the effect of a shift in the dimensionality of the BO_6 linkage on the transport phenomena of electron-doped layered compounds.

Experimental

The stoichiometric compounds of $CaTiO_3$, $Ca_4Ti_3O_{10}$, and $Ca_3Ti_2O_7$ were synthesized by the conventional solid state reaction method. The required amounts of $CaCO_3$ (99.9%) and TiO_2 (99.9%) were mixed in an agate mortar with ethanol. The mixed powder was calcined at 1323 and 1623 K in air with one intermediate grinding. The ground powder was pressed into pellets and fired at 1873 K for 12 hr. The reduced samples $Ca_{n+1}Ti_nO_{3n+1-\delta}$ were obtained by heating pellets in the flowing hydrogen gas atmosphere. The electric furnace with a tungsten heating element was evacuated and filled with dry hydrogen gas through a liquid–nitrogen trap. The condition for reduction to obtain the desired amount of oxygen deficiency δ up to ~0.2 was chosen by changing the heating temperature from 1173 to 1873 K, while the heating time was kept constant at 80 min. The temperature was measured by a W-5%Re/W-26%Re thermocouple and by an optical pyrometer. After the reducing process, the samples were quenched to room temperature in the hydrogen gas flow. The surface of the sample was polished by sandpaper and washed with ethanol. The samples obtained were black, while the very slightly reduced one was gray. They were stable for a few months of storage at room temperature in air. The oxygen vacancy δ was determined by thermogravimetry. Lattice parameters were obtained by least-squares fittings of diffraction lines taken by a Rigaku X-ray diffractometer with a graphite monochrometer. Diffraction data were collected at higher 2θ angles (80–120°) to distinguish $CuK\alpha_1$ lines from $CuK\alpha_2$ lines. High-purity silicon powder was used as an internal standard. The resistivity was measured from room temperature down to 10 K by a

standard four-probe resistivity measurement method. Silver wire (0.1 mm ϕ) leads were attached to the bar-shaped samples via ultrasonic soldering. The dc magnetic susceptibility measurements were made with a Squid magnetometer (Quantum Design MPMS2) over the range 5 to 300 K.

Results and Discussion

Crystal Structure and Dielectric Properties of the $Ca_{n+1}Ti_nO_{3n+1}$ Series

Crystallographic analysis by neutron and X-ray powder diffraction revealed that the crystal structure of the perovskite $CaTiO_3$ is orthorhombic with lattice dimensions a = 5.383 ($\sim\sqrt{2}a_{cubic}$) Å, b = 5.439 ($\sim\sqrt{2}a_{cubic}$) Å, and c = 7.642 ($\sim 2a_{cubic}$) Å (*10*). The orthorhombic distortion of $CaTiO_3$ is caused by the tilting of the TiO_6 octahedra, resulting in the *Pbmn* space group. $CaTiO_3$ transforms to tetragonal at 873 K and to cubic at 1273 K (*11*). The band gap energy at 0 K has been determined by conductivity measurement for a polycrystal to be 3.46 eV (*12*) and by optical measurement for a single crystal to be 3.4 eV (*13*). The crystal symmetries of the n = 2 and 3 compounds, $Ca_3Ti_2O_7$ and $Ca_4Ti_3O_{10}$, have been reported to be body-centered tetragonal (*3*). The detailed physical properties for n = 2 and 3 compounds have not yet been reported. In our study, the X-ray diffraction pattern of both compounds could be indexed on the basis of the *I4/mmm* space group. From the least-squares fittings, we obtained the lattice parameters a = 3.8306(3) Å, c = 19.507(2) Å, and a = 3.8318(3) Å, c = 27.196(9) Å for $Ca_3Ti_2O_7$ and $Ca_4Ti_3O_{10}$, respectively.

A more detailed analysis discriminated the lattice parameter change as a function of the content of the oxygen vacancy δ for the n = 2 compound $Ca_3Ti_2O_{7-\delta}$. This is summarized in Table 1. The results show that the a parameter increases with increasing oxygen vacancy δ, while the c parameter decreases, probably to keep the unit cell volume nearly constant. This may be ascribed to a greater amount of vacancy distribution among the O(2) sites in the *ab* plane than at the O(1) or O(3) site along the c-axis. Gong *et al.* reported a similar result for the $SrTiO_{3-\delta}$ system (*14*). But in the case of $Sr_3V_2O_{7-\delta}$ of the $Sr_{n+1}V_nO_{3n+1-\delta}$ series, the oxygen vacancies are formed at the O(1) site, resulting in a contraction of the a axis and an elongation of the c axis with the increase of δ (*15*).

TABLE I

LATTICE CONSTANTS FOR $Ca_3Ti_2O_{7-\delta}$

δ	a (Å)	c (Å)	V (Å^3)
0.000	3.8306(3)[a]	19.507(2)	286.24
0.001	3.8309(3)	19.509(4)	286.31
0.005	3.8311(4)	19.508(3)	286.33
0.107	3.8321(2)	19.481(1)	286.09

[a] Values in the parentheses denote standard deviations.

The low-temperature dielectric property of the perovskite $CaTiO_3$ is very similar to that of the well-known quantum paraelectric $SrTiO_3$. In pure $SrTiO_3$, the dielectric constant of 2×10^4 becomes temperature independent below 10 K (*16*). In the present study for $CaTiO_3$, a relatively low dielectric constant of 370 was found to be temperature independent below 30 K. As shown in Fig. 1 the dielectric constant ε of $CaTiO_3$ fits seemingly well in Barrett's formula (*17*),

$$\varepsilon(T) = \frac{C}{(T_1/2)\coth(T_1/2T) - T_c}, \quad (1)$$

where $C = 7.7 \times 10^4$, $T_1 = 104$, and $T_c = -159$. For the n = 3 compound $Ca_4Ti_3O_{10}$, $\varepsilon(T)$ also showed quantum paraelectric behaviors. However, in the case of n = 2 compound $Ca_3Ti_2O_7$, the temperature dependence of the dielectric constant showed a diffuse ferroelectric behavior with a low dielectric constant of about 40 below 35 K. Bednorz and Müller (*18*) reported a quan-

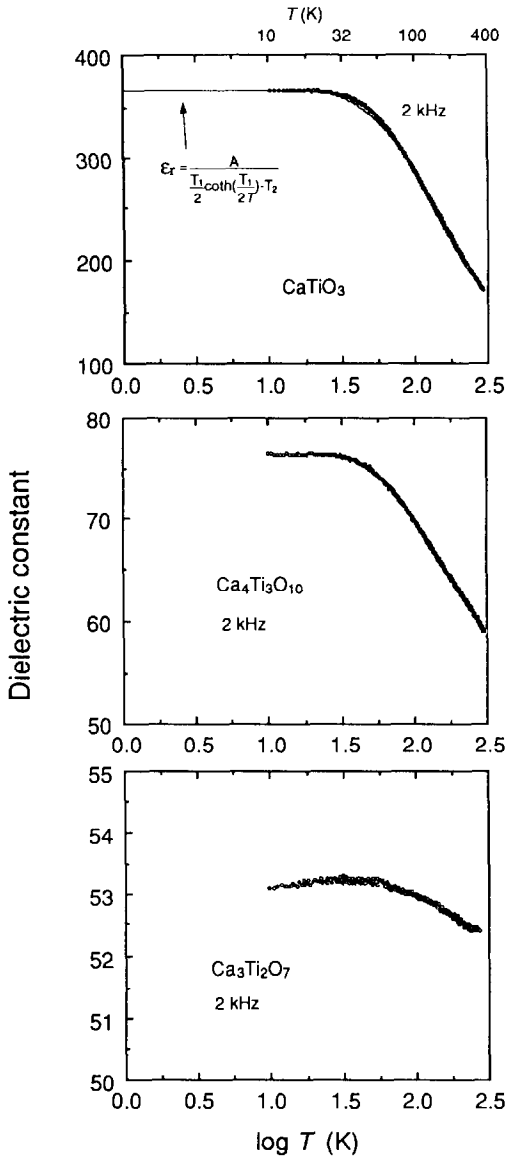

FIG. 1. Temperature dependence of the dielectric constant of the $Ca_{n+1}Ti_nO_{3n+1}$ ceramic samples: $CaTiO_3$ (top), $Ca_4Ti_3O_{10}$ (middle), and $Ca_3Ti_2O_7$ (bottom).

tum ferroelectric behavior of the $Sr_{1-x}Ca_xTiO_3$ system with very small Ca concentrations. They showed that the quantum ferroelectric transition becomes diffuse when the Ca concentration exceeds the value $x = 0.016$. According to their investigation [see Fig. 1 of Ref. (*18*)], the quantum ferroelectric transition temperature in $Sr_{1-x}Ca_xTiO_3$ is limited between 10 and 35 K. This upper limiting temperature ~35 K is approximately equal to and consistent with the quantum paraelectric onset temperature 35 K of $CaTiO_3$ in Fig. 1 of the present paper.

Metallic Resistivity with T^2 Dependence

The layered compounds $CaTiO_3$, $Ca_4Ti_3O_{10}$, and $Ca_3Ti_2O_7$ showed relatively high dielectric constants compared with the other layered Zr, Sn, and Hf compounds (*19*), except for the respective $Sr_{n+1}Ti_nO_{3n+1}$ compounds ($n = 1, 2, 3, \infty$). However, all of the reduced compounds, $CaTiO_{3-\delta}$, $Ca_4Ti_3O_{10-\delta}$, and $Ca_3Ti_2O_{7-\delta}$, showed metallic behavior below room temperature, even when the reduction was very slight. The temperature dependence of the resistivity ρ has been found to be a linear function of T^2. Figure 2a shows the resistivity of reduced $CaTiO_{3-\delta}$ plotted against T^2. Even the very slightly reduced sample of $\delta \sim 0$, for which we estimate the δ to be on the order of few hundreds ppm or less, could fit well to T^2 up to room temperature. Landau and Baber (*20*) pointed out that the T^2 dependence of resistivity is a behavior typical of the strong electron–electron scattering at low temperature in pure metal systems. Mills and Lederer (*21*) showed that the T^2 dependence of ρ is a general feature of a Fermi liquid at a low temperature. In the case of $CaTiO_{3-\delta}$, however, the T^2 dependence of resistivity in Figure 2a can be seen in a rather high temperature range up to 300 K. With the increase in δ, the temperature range of T^2 dependence expands down to the lower temperature. This T^2 dependence of the resistivity is shown by the experimental formula

$$\rho(T) = \rho_M + AT^2, \qquad (2)$$

where the values of the residual resistivity

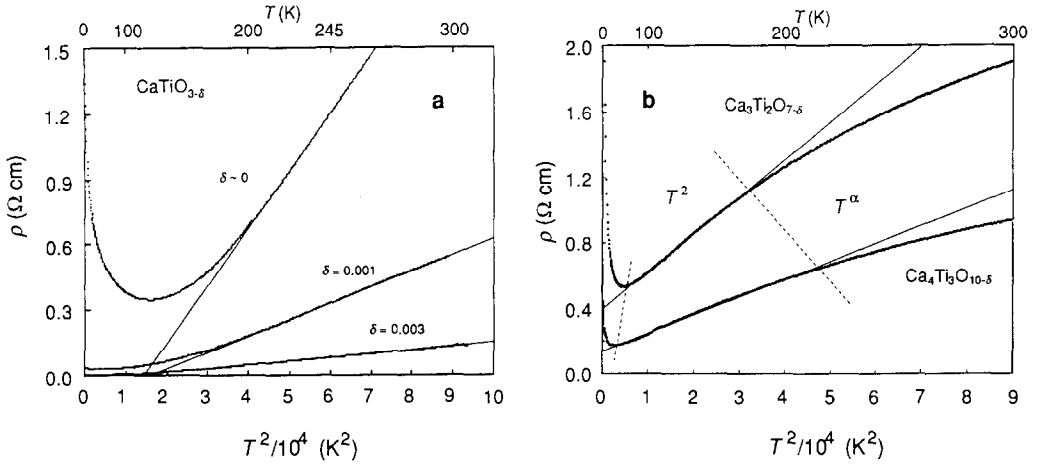

FIG. 2. Electrical resistivity data plotted versus the T^2 law: (a) $CaTiO_{3-\delta}$, with the parameter of oxygen vacancy δ, (b) very slightly reduced $n = 2$ and 3 compounds of $Ca_3Ti_2O_{7-\delta}$ and $Ca_4Ti_3O_{10-\delta}$ ($\delta \leq 0.001$).

ρ_M and the coefficient A of the T^2 term are listed in Table II for $Ca_{n+1}Ti_nO_{3n+1-\delta}$. It is well known that the T^2 dependence of resistivity at low temperature is observed in metallic compounds with highly correlated electron systems. In the case of $CaTiO_{3-\delta}$ the coefficients of the T^2 term were 2.64×10^{-2} and 7.33×10^{-5} mΩ cm/K^2 for $\delta \sim 0$ and $\delta = 0.093$, respectively. The latter value is of the same order as those of the well-known itinerant magnetic compounds $ZrZn_2$, Sc_3In, and V_2O_3 ($A \sim 5 \times 10^{-5}$ mΩ cm/K^2) [Ref. (*22*) and references therein]. The A value of $CaTiO_{3-\delta}$ becomes three orders of magnitude greater than the typical value $A \sim 10^{-5}$ when the reduction is very slight ($\delta < 0.001$).

In the cases of $n = 3$ and $n = 2$ compounds, $Ca_4Ti_3O_{10-\delta}$ and $Ca_3Ti_2O_{7-\delta}$, the resistivities also showed metallic behavior with strong T^2 dependencies. The A values in Eq. (2) show no appreciable difference from those in $n = \infty$ compound $CaTiO_{3-\delta}$. As shown in Table II, the A values of the compounds $Ca_4Ti_3O_{10-\delta}$ and $Ca_3Ti_2O_{7-\delta}$, have the same order as the typical itinerant magnetic compounds, when the contents of oxygen vacancy δ are greater than 0.04. However, in the layered compounds of $n = 2$ or 3, the very slightly reduced samples, ρ did not show T^2 dependence at high temperature as shown in Fig. 2b, but did show T^α dependence with $\alpha < 2$. Mathon (*23*) discussed the temperature dependence of resistivity of weakly ferromagnetic alloys near their critical concentration, giving a result of $T^{5/3}$ dependence. The high-temperature resistivity data of the slightly reduced $n = 2$ and 3 compounds approximately fit the $T^{5/3}$ law. The resistivity of compressed V_2O_3 rises as T^2 up to 50 K and then levels off approximately to a linear rise with T at high temperatures (*24*). Ueda and Moriya (*25*) have developed a theory of electrical and thermal resistivities of weakly and nearly ferromagnetic metals, which show T^2 dependence at very low temperature with a large coefficient, $T^{5/3}$ dependence near and above T_c, and T^1 or T^0 dependence at high temperature. According to their study, the large coefficient of the T^2 term at low temperature resistivity originated from spin fluctuations, which is characteristic of weak itinerant ferromagnetic metals.

TABLE II

PARAMETERS OBTAINED FROM THE ELECTRICAL CONDUCTIVITY DATA FOR THE $Ca_{n+1}Ti_nO_{3n+1-\delta}$ SYSTEM

δ	$\rho_{300\,K}$ (mΩ cm)	ρ_M[a] (mΩ cm)	A[a] (mΩ cm K^{-2})	T_{MNM} (K)	T^*[b] (K)	B[c] ($K^{-1/4}$)	ρ_0[d] (mΩ cm)	E_a[d] (meV)
			$Ca_3Ti_2O_{7-\delta}$ (n = 2)					
<0.001	1902	407	2.22×10^{-2}	67	25.1	35300	3.2	3.91
0.005	253	65.3	2.26×10^{-3}	100	33.3	6092	6.9	3.81
0.042	80.4	11.1	7.98×10^{-4}	63	31.3	54	6.7	1.22
0.104	49.3	6.09	5.00×10^{-4}	54	27.6	32	3.8	0.88
0.260	30.6	2.37	3.22×10^{-4}	30	—	—	—	0.12
			$Ca_4Ti_3O_{1-\delta}$ (n = 3)					
<0.001	950	138.4	1.12×10^{-2}	58	31.6	863	21.0	1.47
0.048	87.5	24.8	7.05×10^{-4}	55	23.8	2.1	17.2	0.37
0.113	42.1	3.42	4.33×10^{-4}	35	13.2	0.33	3.3	0.16
0.200	14.2	1.70	1.44×10^{-4}	26	—	—	1.9	0.03
0.232	4.92	0.65	0.49×10^{-4}	45	13.2	3.7	0.4	0.32
			$CaTiO_{3-\delta}$ (n = ∞)					
<0.001	1975	−381.0	2.64×10^{-2}	125	71.4	334	140.9	5.75
0.001	542	−114.7	7.43×10^{-3}	61	32.3	29	12.0	0.58
0.003	132	19.8	1.70×10^{-3}	Metallic down to 10 K				
0.093	6.75	0.11	0.73×10^{-4}	Metallic down to 10 K				

[a] $\rho(T) = \rho_M + AT^2$.
[b] Crossover temperature from activation type to variable range hopping.
[c] $\rho(T) = \rho_0 \exp(B/T^{1/4})$
[d] $\rho(T) = \rho_0 \exp(E_a/kT)$

Metal–Nonmetal Transition and Nonmetallic Conductivity

Figure 3 shows the resistivity data of very slightly reduced $n = 2$ compound $Ca_3Ti_2O_7$. Below 70 K the resistivity shows a semiconducting behavior with a sharp increase, which gives a vanishing conductivity at 0 K. In the previous section, we showed a T^2 dependence with a large coefficient in resistivity of the metallic phases in the reduced $Ca_{n+1}Ti_nO_{3n+1-\delta}$ compounds. We assumed that the electron–electron interaction provides the principal driving force of the metal–nonmetal transitions. The metal–nonmetal transition temperature is depressed smoothly with increasing δ. As shown in Table II, the transition temperatures depend strongly on oxygen deficiency

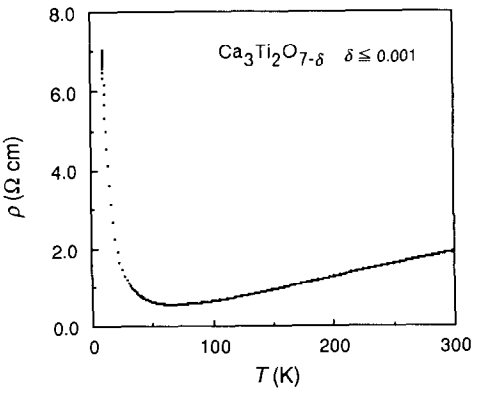

FIG. 3. Electrical resistivity of the slightly reduced $Ca_3Ti_2O_{7-\delta}$ ($\delta \leq 0.001$), showing metal–nonmetal transition at 70 K and zero conductivity at 0 K.

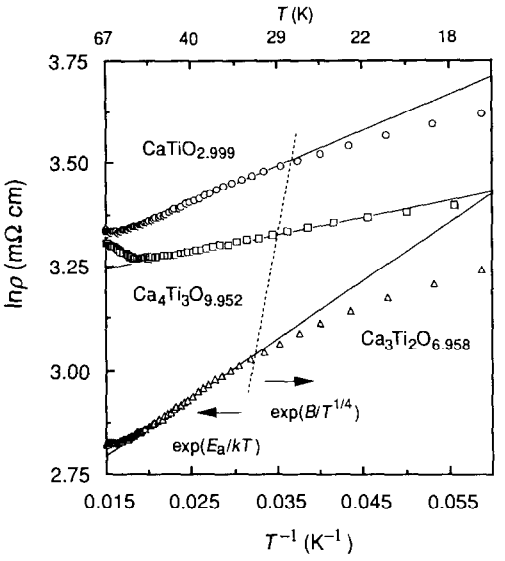

FIG. 4. Logarithmic resistivity versus reciprocal temperature of $Ca_3Ti_2O_{6.958}$, $Ca_4Ti_3O_{9.952}$ and $CaTiO_{2.999}$.

δ rather than the structural parameter n of the $Ca_{n+1}Ti_nO_{3n+1-\delta}$ compounds. The metal–nonmetal transition occurs below 120 K, that is, with a thermal stimulation lower than 10 meV. The small thermal energy contributions to the total free energy produce qualitative changes in the nature of the electron states on the scale of electron volts (3.4 eV for $CaTiO_3$), which was well understood for systems like V_2O_3 [see review paper of Ref. (*26*)].

Figure 4 shows the logarithmic resistivities normalized with the values of 10 K vs the reciprocal temperature for the very slightly reduced compounds $CaTiO_{3-\delta}$, $Ca_4Ti_3O_{10-\delta}$, and $Ca_3Ti_2O_{7-\delta}$. From the linear relation shown in Fig. 4, the activation energy E_a

$$\rho(T) = \rho_0 \exp(E_a/kT) \qquad (3)$$

can be obtained, and the results are shown in Table II. The activation energies of the series compounds have values smaller than a few meV, which decrease to the order of 10^{-4} eV with an increasing oxygen vacancy, i.e., with an increasing donor concentration. The energy value of an order of 10^{-4} eV does not correspond to an activation across the energy gap from the valence band, but does correspond to an activation from a donor level introduced by the oxygen deficiency. Mott (*27*) showed that if the donor electron forms a hydrogen-like orbital with a radius of $\alpha_H = h^2\varepsilon/m^*e^2$ the donor level E_d can be expressed as

$$E_d = m^*e^4/2h^2\varepsilon^2. \qquad (4)$$

This equation was derived for the system with a dielectric constant $\varepsilon \geq 100$. If we apply the above equation to the $Ca_{n+1}Ti_nO_{3n+1}$ compounds, the hydrogen-like donor level E_d is calculated to be on the order of 10^{-4} eV by putting m^* as normal electron mass. The E_a values with respective dielectric constants agree well with the values obtained from Eq. (3) in order of magnitude. On the lower temperature side of Fig. 4, the plots deviate from linear relations. This implies that the activation energy E_a is temperature dependent, which may be caused

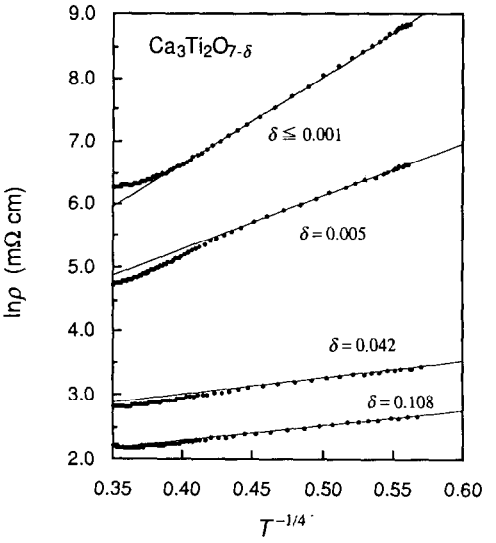

FIG. 5. The linear dependence of ln ρ versus $T^{-1/4}$ for $Ca_3Ti_2O_{7-\delta}$, verification of the $T^{-1/4}$ law.

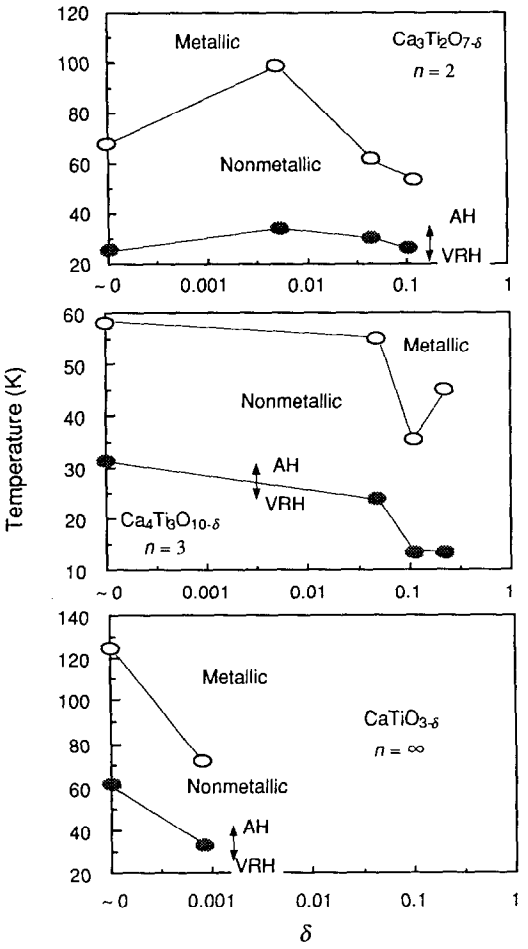

FIG. 6. Plot of the metal–nonmetal transition temperature and the crossover temperature from activation type (AH) to variable range hopping (VRH): $Ca_3Ti_2O_{7-\delta}$ (top), $Ca_4Ti_3O_{10-\delta}$(middle), and $CaTiO_{3-\delta}$ (bottom). Note that the zero point of the x axis is shifted arbitrarily.

by so-called "variable range hopping" (*27*), characteristic of a weakly localized system.

$$\rho(T) = \rho_0 \exp(B/T^{1/4}) \qquad (5)$$

Figure 5 shows the data fitted to the expression of the variable range hopping in Eq. (5) for $n = 2$ compound $Ca_3Ti_2O_{7-\delta}$. The data fit well to Mott's $T^{-1/4}$ law below some low temperature regions ($T < T^*$). The results of $T^{-1/4}$ fittings in Table II show that the B values in Eq. (5) significantly depend on the oxygen deficiency δ, ranging from 10^4 to 10 for $\delta \sim 0$ to $\delta = 0.104$, respectively. Values of the parameter B and the approximate onset temperature T^* for $Ca_3Ti_2O_{7-\delta}$, $Ca_4Ti_3O_{10-\delta}$, and $CaTiO_{3-\delta}$ are also given in Table II. It is obvious that the characteristic energy for the hopping state, B, decreases with increasing δ. When the characteristic energy B becomes nearly zero, the metallic phase is stabilized at all temperatures. From this point of view, it is reasonable to expect that the crossover temperature T^* will be closely related to the metal–nonmetal transition temperature T_{MNM}. When we plotted T^* and T_{MNM} in Fig. 6 as a function of the oxygen deficiency δ for the $Ca_{n+1}Ti_nO_{3n+1-\delta}$ compounds, we could find a similar δ dependency between the onset temperature T^* and the metal–nonmetal transition temperature T_{MNM}.

The dc magnetic susceptibility data for the system are shown in Fig. 7. They are nearly temperature independent, especially for the very slightly reduced system. The magnetic susceptibility data obeyed the

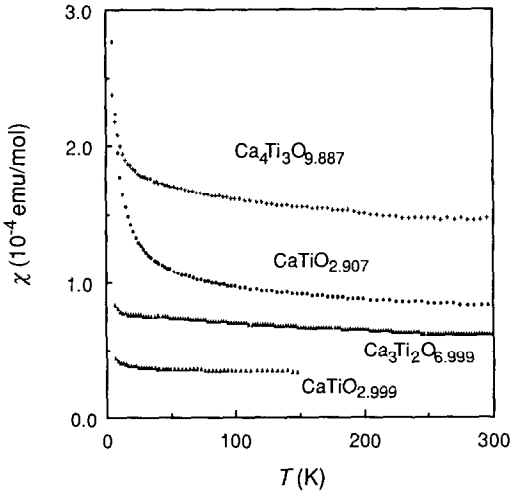

FIG. 7. The temperature dependence of the dc magnetic susceptibility for the $Ca_{n+1}Ti_nO_{3n+1-\delta}$ system.

Curie–Weiss law, including temperature-independent paramagnetic contribution. The temperature-independent terms were 33×10^{-6} (emu/mole) for $CaTiO_{2.999}$ and 127×10^{-6} (emu/mole) for $Ca_4Ti_3O_{9.887}$. These values showed a strong dependency on the oxygen vacancy δ, but little dependency on the structural parameter n. The heavily reduced compounds show a sharp increase in magnetic susceptibility below a few tens kelvin in Fig. 7. Since these compounds are strongly electron-correlated metallic ones with large T^2 terms, the sharp upturns in Fig. 7 might be ascribed to a localization of the donor electron at an oxygen vacancy. According to Mott and Davis (*27*), the increase in oxygen vacancy in $Ca_{n+1}Ti_nO_{3n+1-\delta}$ yields a hydrogen-like atomic radius smaller than the nearest metallic ion separation, resulting in a localization of the donor electrons. The driving force for this localization is considered to come from the intraatomic Coulomb potential. Unfortunately, since our resistivity measurements were performed only in a limited temperature range (10–300 K), we could not observe the opening of the Coulomb gap which may appear at very low temperature (*28*).

The metal–nonmetal transition can be frequently explained by Mott–Hubbard transition, proposed originally by Gutzwiller and by Brinkmann and Rice [see Ref. (*26*) and references therein]. The insulating state of the half-filled band ($Ti^{3+} = 3d^1$) can be described as an electron state of an atom-like wave function, including electron–electron interaction. In order to explain the transport phenomena of the $Ca_{n+1}Ti_nO_{3n+1-\delta}$ system, we propose the density of states depicted in Fig. 8. The vacant upper Hubbard band overlaps the lower part of the conduction band, including its mobility edge and its tail, where the states are localized. Nonmetallic conduction can be realized by activation (σ_1) from the filled lower Hubbard band above the mobility edge or by variable range hopping (σ_2) to the localized states of the tail below the mobility edge. The metallic state can be understood by picturing the Mott–Hubbard transition; the large T^2 term and Paulli paramagnetism for the $Ca_{n+1}Ti_nO_{3n+1-\delta}$ system support the picture. However, in this study we did not show effective mass enhancement at the transition, which is typical of the Mott–Hubbard transition. A very large dielectric constant at low temperature in the $Ca_{n+1}Ti_nO_{3n+1-\delta}$ system suggests that the charge carriers are polarons, as is well exemplified in $SrTiO_3$, and different transport mechanisms, i.e., a polaron band and polaron hopping regime, can be applied (*29*). But it is not a simple matter to classify a polaron material.

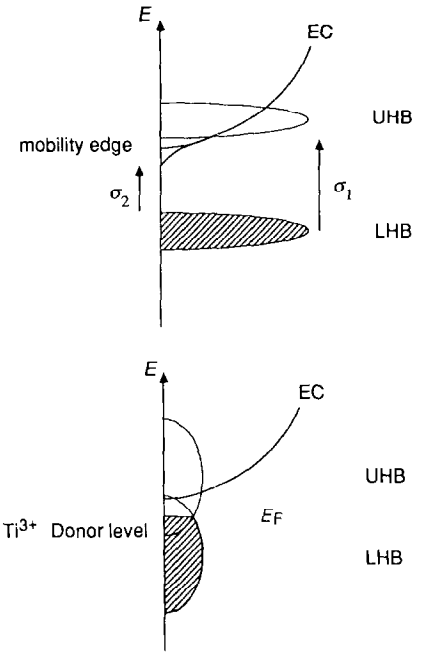

FIG. 8. Possible density of states $N(E)$ for the reduced calcium titanate. (Top) Nonmetallic conduction can be realized by activation (σ_1) from the filled lower Hubbard band above the mobility edge or by variable range hopping (σ_2) to the localized states of the tail below the mobility edge. (Bottom) The metallic state can be realized by the overlap of the bands at high temperature.

Summary

In summary, the dielectric properties indicated a so-called quantum paraelectric behavior with strong dependence on the structural parameter n in the $Ca_{n+1}Ti_nO_{3n+1}$ system (n = 2, 3, and ∞). The electrical conductivity of the reduced $Ca_{n+1}Ti_nO_{3n+1-\delta}$ system showed metal–nonmetal transition as a function of temperature below 120 K. The room temperature resistivity was in the range 10^3–10^0 mΩ cm for $\delta \sim 0$ and $\delta \sim 0.2$, respectively, and showed a stronger dependency on δ than on the layer parameter n. The metallic resistivity obeyed the T^2 law up to room temperature with a large coefficient A. In the slightly reduced n = 2 and 3 compounds, the resistivity showed a nearly $T^{5/3}$ dependence. The nonmetallic conductivity at low temperature can be explained by activation-type hopping and by the mechanisms of variable range hopping.

References

1. J. F. Shooley, W. R. Holser, and M. L. Cohen, *Phys. Rev. Lett.* **12,** 474 (1964).
2. S. N. Ruddlesdon and P. Popper, *Acta Crystallogr.* **10,** 538 (1957); **11,** 541 (1958).
3. R. S. Roth, *J. Res. NBS* **61,** 437 (1958).
4. J. B. Goodenough and J. M. Longo, "Landolt-Börnstein Tabellen," Vol. 111/4a, Springer-Verlag, Berlin (1970); J. B. Torrance and P. Lacorro, *J. Solid State Chem.* **90,** 168 (1991).
5. J. B. Goodenough, *Prog. Solid State Chem.* **5,** 145 (1971).
6. P. Ganguly and C. N. R. Rao, *J. Solid State Chem.* **53,** 193 (1984); C. N. R. Rao, P. Ganguly, K. K. Singh, and R. A. Mohan Ram, *J. Solid State Chem.* **72,** 14 (1988); M. Cyrot *et al., J. Solid State Chem.* **85,** 321 (1990).
7. P. D. Edwards and C. N. R. Rao (Eds.), "The Metallic and Nonmetallic States of Matter," Taylor & Francis, London/Philadelphia (1985).
8. N. Tsuda, K. Nasu, A. Yanase, and K. Siratoti, "Electronic Conduction in Oxides," Springer-Verlag, Berlin (1990); K. H. Kim, K. H. Yoon, and J. S. Choi, *J. Phys. Chem. Solids* **46,** 1061 (1985).
9. G. J. McCarthy, W. B. White, and R. Roy, *J. Am. Ceram. Soc.* **52,** 463 (1969).
10. H. Koopmans, G. van de Valde, and P. Gellings, Acta Crystallogr. C **39,** 1323 (1983); M. Ceh, D. Kolar, and L. Golic, *J. Solid State Chem.* **68,** 68 (1987).
11. L. C. Walters and R. E. Grace, *J. Phys. Chem. Solids* **28,** 824 (1967).
12. A. Linz and K. Herrington, *J. Chem. Phys.* **28,** 824 (1958).
13. U. Balachandran, B. Odekirk, and N. G. Error, *J. Solid State Chem.* **41,** 185 (1982); G. A. Cox and R. H. Trdgold, *Br. J. Appl. Phys.* **18,** 37 (1967).
14. W. Gong, H. Yun, Y. B. Ning, J. E. Greedan, W. R. Datars, and C. V. Starger, *J. Solid State Chem.* **90,** 320 (1991).
15. M. Itoh, M. Shikano, H. Kawaji, and T. Nakamura, *Solid State Commun.*, in press.
16. K. A. Müller and H. Buckard, *Phys. Rev. B* **19,** 3593 (1979).
17. J. H. Barret, *Phys. Rev.* **86,** 118 (1952).
18. J. G. Bednorz and K. A. Müller, *Phys. Rev. Lett.* **52,** 2289 (1984).
19. Unpublished research by the authors.
20. L. D. Landau, *Phys. Z. Sowjetunion* **3,** 664 (1933); W. G. Baber, *Proc. R. Soc. A* **158,** 383 (1936).
21. D. L. Mills and P. Lederer, *J. Phys. Chem. Solids* **27,** 1805 (1966).
22. T. Ohtani and S. Onoue, *J.Solid State Chem.* **59,** 324 (1985).
23. J. Mathon, *Proc. R. Soc. A* **306,** 355 (1968).
24. D. B. McWhan and T. M. Rice, *Phys. Rev. Lett.* **22,** 887 (1969).
25. K. Ueda and T. Moriya, *J. Phys. Soc. Jpn.* **39,** 605 (1975).
26. J. Spalek, *J. Solid State Chem.* **88,** 70 (1990), and other review papers in this volume titled "Transition-Metal Compounds: Insulators, Metals, Superconductors."
27. N. F. Mott and E. A. Davis, "Electronic Processes in Non-Crystalline Materials," Clarendon Press, Oxford (1979).
28. A. L. Efros and B. I. Schklouvskii, *J. Phys. C: Solid State Phys.* **8,** L49 (1975).
29. J. M. Honig, *IBM J. Res. Develop.* **14,** 232 (1970).